fire

MDPI

Article

An Air–Ground Collaborative Emergency Material Dispatch Method for Wildfires in Dynamic Time-Varying Environments: A Case Study of the High-Altitude Plateau Region in Western China

Rundong Wang [1,*], Lanxi Xu [1,*], Yuanjing Huang [2], Weijun Pan [3] and Zirui Yin [4]

[1] College of Air Traffic Management, Civil Aviation Flight University of China, Guanghan 618307, China
[2] Air Traffic Control Center, Civil Aviation Flight University of China, Guanghan 618307, China; hyj@cafuc.edu.cn
[3] Flight Technology and Flight Safety Research Base of the Civil Aviation Administration of China, Civil Aviation Flight University of China, Guanghan 618307, China; wjpan@cafuc.edu.cn
[4] School of Transportation and Logistics, Southwest Jiaotong University, Chengdu 610031, China; yin@my.swjtu.edu.cn
* Correspondence: random@cafuc.edu.cn (R.W.); stxlx@foxmail.com (L.X.)

Abstract

Wildfires in plateau and mountainous regions are increasingly destructive, often disrupting ground transportation networks and severely constraining emergency logistics, while unmanned aerial vehicles (UAVs) remain limited by payload capacity. To address this challenge, this study proposes an air–ground collaborative emergency material dispatch method for dynamic, time-varying wildfire environments. A multi-layer spatiotemporal network model is developed by incorporating key uncertainties, including fire spread and meteorological fluctuations, into dynamic parameters, and a multi-objective mixed-integer programming framework is established to jointly optimize emergency response time, total dispatch cost, and rescue fairness. To solve the resulting high-dimensional dynamic rescheduling problem, a Fast Ant Colony Optimization-Genetic Algorithm (FACO-GA) integrated with a rolling horizon mechanism is designed. Simulation results under Level 1–10 dynamic perturbations show that, compared with conventional standalone algorithms (GA and ACO), the proposed method demonstrates markedly better robustness and computational efficiency, reducing the extreme average rescheduling response time to 6.80 s, while maintaining a Hypervolume (Hv) retention rate of 96.30% and limiting the Spacing (Sp) change rate to 4.15%. These findings indicate that the proposed approach can effectively overcome computational bottlenecks and provide an adaptive decision-support framework for emergency logistics dispatch in complex wildfire scenarios. Furthermore, comprehensive ablation studies and sensitivity analyses validate the structural necessity of the rolling horizon and ACO modules, ensuring the algorithm's parameter robustness under extreme stochastic perturbations.

Keywords: wildfire; emergency material dispatch; air–ground collaborative rescue; multi-objective optimization; FACO-GA

Check for updates

Academic Editor: Grant Williamson

Received: 29 March 2026
Revised: 23 June 2026
Accepted: 3 July 2026
Published: 5 July 2026

Copyright: © 2026 by the authors. Licensee MDPI, Basel, Switzerland. This article is an open access article distributed under the terms and conditions of the Creative Commons Attribution (CC BY) license.

1. Introduction

Wildfires have become increasingly frequent and destructive under the combined effects of global climate change, prolonged drought, and extreme weather, posing growing

threats to ecological security, infrastructure, and human life. In plateau and mountainous regions, wildfire disasters are further amplified by complex topography, fragile transportation networks, and rapidly changing local meteorological conditions. Once a wildfire occurs, steep terrain, road damage, smoke obstruction, and shifting wind fields can quickly interrupt ground transportation and isolate affected zones, substantially reducing the efficiency of emergency logistics and rescue operations. In this context, timely and reliable material dispatch is essential for supporting front-line firefighting, medical aid, and post-disaster emergency response. Compared with conventional ground-based delivery, unmanned aerial vehicles (UAVs) offer rapid deployment, flexible mobility, and reduced dependence on damaged road infrastructure, making them particularly suitable for emergency operations in inaccessible mountainous wildfire areas. Therefore, an air–ground collaborative dispatch mode that combines the long-range, high-capacity advantages of ground vehicles with the flexible "last-mile" delivery capability of UAVs has emerged as a promising solution for wildfire emergency logistics.

For example, during the catastrophic 2019 Muli forest fire in Sichuan, China, and the devastating 2019–2020 bushfires in Australia, sudden wind shifts and rugged mountainous terrain caused severe ground route blockages. Firefighters were frequently isolated in "rescue islands" without timely supply replenishment, leading to tragic casualties and delayed containment. If an air–ground collaborative system had been deployed during these crises—where trucks safely transported supplies to the edge of impassable zones and UAVs bypassed the blocked terrain to deliver critical materials (e.g., water, emergency medical kits)—the emergency intervention would have been significantly more efficient, and front-line safety would have been vastly improved. However, emergency material dispatch in plateau and mountainous wildfire scenarios differs fundamentally from conventional logistics problems because the disaster environment is highly dynamic and time-varying. Wildfire spread, wind direction changes, meteorological fluctuations, road accessibility, and emergency demand can all evolve rapidly over short time intervals, causing continuous changes in route availability, node conditions, and vehicle performance. Although existing studies on emergency logistics, truck–UAV collaboration, and dynamic vehicle routing have achieved valuable progress, most still rely on static or simplified deterministic assumptions and primarily focus on minimizing travel time or economic cost. As a result, they often fail to capture the continuous evolution of wildfire disasters, the complex coupling constraints of heterogeneous vehicle coordination, and the multi-objective trade-offs among response timeliness, dispatch cost, and rescue fairness. These limitations become more pronounced in high-plateau wildfire environments, where traditional models and standalone algorithms are prone to dimensional explosion, computational inefficiency, and degradation in solution quality under dynamic perturbations. To address these gaps, this study proposes an air–ground collaborative emergency material dispatch method under dynamic time-varying conditions. Specifically, a multi-layer spatiotemporal network is constructed by embedding wildfire spread, road damage, and meteorological variation into the dispatch process, and a hybrid optimization framework is developed to support efficient dynamic rescheduling in complex emergency environments.

To address these gaps, the specific objectives and contributions of this study are formulated as follows:

- Objective 1 (Modeling Environmental Dynamics): To establish an air–ground collaborative emergency material dispatch model for wildfire scenarios that explicitly quantifies key environmental uncertainties—such as wildfire spread, damaged road capacity, and meteorological variation—into dynamic parameters.

- Objective 2 (Multi-Objective Optimization): To develop a multi-objective mixed-integer programming framework that jointly optimizes emergency response time, total dispatch cost, and rescue fairness, providing a comprehensive decision-making basis.
- Objective 3 (Algorithm Design and Dynamic Rescheduling): To design a Fast Ant Colony Optimization-Genetic Algorithm (FACO-GA) integrated with a rolling horizon mechanism, enabling rapid local adjustment and overcoming computational bottlenecks in high-dimensional dynamic rescheduling.

2. Related Work

With the frequent occurrence of natural disasters and emergencies, emergency material dispatch has become an important research direction in the field of emergency management. This section reviews the current research status from three aspects: emergency resource dispatch, air–ground collaborative delivery, and dynamic optimization methods.

2.1. Emergency Resource Dispatch

The core objective of emergency resource dispatch is to quickly and efficiently deliver rescue materials to affected areas after a disaster. Early research mainly focused on optimizing resource dispatch for a single transportation mode. Wang et al. [1] addressed the emergency material dispatch problem from multiple depots to multiple disaster sites, establishing an optimization model aimed at maximizing reliability and minimizing costs, and balanced the two objectives by introducing the concept of an ideal point. Feng and Cui [2] conducted a systematic review of 3678 papers in the emergency response field, pointing out that optimization and demand are the most focused research topics in this area. On a global scale, the optimization of emergency resource dispatch forms the core of humanitarian logistics and disaster operations management. Foundational international studies, such as the comprehensive framework proposed by Altay and Green [3], have long established the critical need for integrating operational research methodologies into pre- and post-disaster phases. In the specific context of wildfire management, international researchers have developed advanced spatial optimization models. For example, Duff and Tolhurst [4] pioneered operational resource allocation models that dynamically align suppression resources with shifting fire spread perimeters, providing a strong theoretical basis for international wildfire logistics. In terms of emergency restoration of distribution systems, Lei et al. [5] proposed a resilient post-disaster recovery method that collaboratively schedules repair crews and mobile power sources, significantly enhancing the recovery capability of the distribution system through coupled optimization of transportation and power networks. Xu et al. [6] considered the impact of traffic congestion on mobile emergency resource dispatch and used a cell transmission model to describe the dynamic traffic assignment problem, achieving efficient restoration of critical loads. Targeting extreme weather disasters, Qin et al. [7] proposed a two-stage dispatch method for distribution network emergency resources, enhancing grid survivability through pre-disaster prevention and post-disaster coordinated dispatch.

Cross-regional collaborative dispatch is another important research direction for emergency resources. Qiu et al. [8] established a system dynamics model based on a multi-agent game, revealing the crucial role of high-level supervision and incentive mechanisms in promoting cross-regional collaborative dispatch of emergency supplies. Jiang et al. [9] designed a three-level collaborative mechanism including total cost synergy, investment conversion synergy, and cross-regional dispatch synergy, effectively balancing the supply and demand of inter-regional emergency resources. Chen et al. [10] built a three-level multimodal transportation network model considering demand and route reliability, improving the reliability of cross-regional dispatch through coordinated transport of aviation, rail-

way, and highway systems. Furthermore, researchers have proposed various specialized dispatch methods for specific disaster scenarios. Wu et al. [11] developed a resource-constrained emergency scheduling integer programming model for priority areas in forest fires, accurately solving large-scale instances involving 100 fire points and 30 fire brigades within 1 min. Yang et al. [12] constructed an emergency logistics system for wildland fire suppression based on fire spread prediction, optimizing resource allocation and vehicle routing by forecasting disaster evolution. For maritime search-and-rescue scenarios, Ma et al. [13] combined LSTM for predicting accident numbers with the K-means algorithm for identifying accident black spots, establishing a multi-objective emergency resource allocation optimization model.

2.2. Air–Ground Collaborative Delivery

With the rapid development of unmanned aerial vehicle (UAV) technology, the air–ground collaborative delivery model has gradually become a vital tool in emergency logistics. The theoretical foundation of air–ground collaborative delivery—often recognized internationally as the "Flying Sidekick Routing Problem" (FSRP) or the "Traveling Salesman Problem with Drone" (TSP-D)—was largely established by seminal international works. Murray and Chu [14] first formulated the mathematical framework for routing a truck paired with a drone, demonstrating significant savings in delivery time. Similarly, Agatz et al. [15] developed exact and heuristic approaches for the TSP-D, expanding its application viability. Subsequent international reviews, such as those by Macrina et al. [16], have tracked the evolution of this paradigm to include multi-drone operations and time-window constraints. However, applying these static theoretical frameworks to highly unpredictable and time-critical disaster scenarios remains an emerging frontier that this study aims to address. Wang et al. [17] systematically reviewed the key technologies and future trends of UAV–ground vehicle collaborative delivery in emergency response, noting that the field has evolved from single-machine applications to intelligent multi-mode collaborative systems, demonstrating significant advantages in medical supply delivery, disaster rescue, and search-and-rescue operations. Regarding collaborative delivery models, Li et al. [18] constructed a vehicle–UAV collaborative path optimization model considering time windows, start-up costs, waiting costs, and penalty costs, reducing total costs by 39.2% compared to single delivery modes. Qi et al. [19] designed a multi-layer, multi-stage encoding and decoding strategy based on a three-learning strategy particle swarm optimization algorithm for customer-priority pickup and delivery problems, reducing total costs by 14.86% in a 50-node scenario. Ghaffar et al. [20] proposed a vehicle–UAV integrated routing optimization method combining DBSCAN clustering and an improved artificial bee colony algorithm for the emergency delivery of medical supplies.

Multi-UAV collaborative scheduling is key to improving delivery efficiency. Pan et al. [21] built a multi-aircraft collaborative scheduling optimization model for forest fire rescue, using the NSGA-II algorithm and weighted TOPSIS method to find the optimal scheduling scheme, thereby improving aircraft utilization while ensuring rescue timeliness. Lin et al. [22] studied a multi-truck and multi-UAV collaborative transportation system, achieving efficient medical supply delivery through a hybrid particle swarm optimization algorithm. Gong et al. [23] proposed a priority-based multi-stage UAV collaborative emergency material scheduling system and designed a hybrid algorithm TGA-BB integrating tabu search and branch-and-bound, which reduced the average response time by 52.37%. The joint optimization of path planning and resource allocation is the core issue in air–ground collaborative delivery. Feng and Cao [24] proposed a neural network-based path planning framework for air–ground collaborative logistics, integrating K-means clustering and a three-stage neural architecture that considers dynamic weather adaptability, reducing

costs by 21.3%. Liu et al. [25] established a mixed-integer linear programming model for joint UAV–truck scheduling in last-mile logistics distribution, optimizing delivery times via a three-stage solution scheme.

2.3. Dynamic Optimization Methods

Dynamic time-varying characteristics are a significant feature of emergency scenarios, and scheduling optimization methods that consider these factors have received widespread attention. The transition from static routing to dynamic vehicle routing problems (DVRP) has been a major focus in international operations research. As systematically reviewed by Pillac et al. [26] and further expanded by Psaraftis et al. [27], dynamic optimization requires algorithms that can adapt in real time to newly revealed information, such as new demand requests or travel time variations. While these global studies highlight the efficacy of metaheuristics and rolling horizon frameworks in managing dynamic logistics, their application has predominantly centered on commercial transportation. Adapting these dynamic metaheuristics to the extreme uncertainties of wildfire spread necessitates specialized structural redesigns, such as the integrated local repair mechanism proposed in our FACO-GA. Luscombe and Kozan [28] proposed a dynamic resource scheduling framework for emergency departments, integrating dispatch heuristics, disjunctive graph methods, and meta-heuristic searches, enabling dynamic schedule updates within 2 s of information renewal. Chai et al. [29] optimized traffic emergency resource scheduling through dynamic route time estimation by accounting for queuing delays caused by traffic accidents, enhancing rescue response efficiency. Regarding disaster prediction and dynamic scheduling, Pi et al. [30] proposed an emergency resource dispatch strategy for ice disasters based on pre-disaster prediction and dynamic scheduling; by utilizing a fast Newman algorithm for community clustering and introducing mobile energy storage and water trucks, user satisfaction increased by 24.73%. Ye et al. [31] developed a marine oil-spill emergency response system based on dynamic simulation and enhanced particle swarm optimization, significantly improving emergency response decision-making capabilities through process simulations of resource scheduling, oil weathering, and oil clearance. Intelligent optimization methods such as reinforcement learning are increasingly being applied in emergency resource scheduling. Dabrowski and Walczak [32] systematically reviewed the application of reinforcement learning in optimizing emergency resource dispatch strategies, identifying state-space design, action-space definition, reward-function design, and environmental modeling as key factors affecting model performance. In space–air–ground integrated networks, Liu et al. [33] utilized a multi-agent deep deterministic policy gradient algorithm to jointly optimize UAV 3D trajectories and resource scheduling, achieving a balance between throughput and energy consumption. Qin et al. [34] combined the AVOA and MADDPG algorithms to jointly optimize content caching, resource allocation, and UAV trajectories in air–ground integrated networks, significantly improving system energy efficiency.

2.4. Research Gaps

To clarify the characteristics of the aforementioned studies and highlight the innovations of our proposed method, a comprehensive summary is provided in Table 1.

In summary, existing studies have made rich achievements in emergency resource dispatch, air–ground collaborative delivery, and dynamic optimization methods. However, most research focuses on static or quasi-static scenarios, with insufficient consideration given to the dynamic and time-varying characteristics of disaster evolution. Research on air–ground collaborative delivery mostly targets conventional logistics, while studies tailored specifically to emergency scenarios remain relatively sparse. Furthermore, the optimization methods applied are predominantly heuristic algorithms or traditional re-

inforcement learning, meaning their real-time performance and robustness in complex dynamic environments still require improvement. Therefore, addressing the air–ground collaborative emergency material dispatch problem under dynamic time-varying characteristics, this paper establishes a comprehensive optimization model that considers disaster evolution, traffic conditions, and resource constraints, and designs a highly efficient solving algorithm to enhance the timeliness and effectiveness of emergency responses.

Table 1. Summary of literature review and research gaps.

Research Category	Representative Studies	Scenario Assumption	Optimization Focus	Methodological Characteristics
Emergency Dispatch	[1,8–13]	Mostly Static/Quasi-static	Reliability, Cost, Timeliness	Traditional OR/Heuristics
Air–Ground Collaboration	[14,15,18,20,21,23–25]	Commercial/Standard Logistics	Routing Efficiency	Heuristics (e.g., GA, PSO, ABC)
Dynamic Optimization	[26–28,30,31,33,34]	Specific Disaster Scenarios	Real-time Adaptability	Metaheuristics, Reinforcement Learning
This Paper	Proposed Method	Dynamic, Time-Varying Wildfire	Time, Cost, Fairness	Rolling Horizon + FACO-GA

3. Materials and Methods

3.1. Problem Description and Application Scenario

Wildfire emergency response in high-plateau mountainous regions is often confronted with multiple practical challenges, including rugged terrain, limited ground accessibility, and dynamic disaster evolution. As a result, reliance on a single mode of transportation is highly susceptible to road-network paralysis, leading to the formation of rescue islands. To address this, the air–ground collaborative dispatch model—integrating the heavy-load, long-distance capabilities of ground trucks with the agile, terrain-independent advantages of unmanned aerial vehicles (UAVs)—has emerged as a critical operational strategy.

In the typical application scenario of this study, the emergency response system comprises a central material reserve depot, multiple available temporary air transit points, and a set of geographically dispersed fire-delivery points with dynamically changing demands. The rescue tasks are executed by a heterogeneous fleet consisting of medium trucks and UAVs. The environment is dynamically time-varying, characterized by fire spread, meteorological fluctuations, and changing airspace availability. The decision-making objective is to plan optimal spatiotemporal paths for each vehicle under multiple constraints (e.g., dynamic safety intervals, endurance, and payload limits) to minimize response time and system cost while maximizing rescue fairness.

To provide a clearer illustration of the application scenario and support the understanding of the collaborative routing problem, Figure 1 presents a schematic diagram of the air–ground collaborative material dispatch process in the disaster-affected area.

In this collaborative framework, medium trucks function not only as primary ground transport vehicles but also as mobile launching and recovery platforms for the UAVs. Specifically, a truck carries its paired UAV to a designated and accessible road node. From there, the UAV takes off, flies over impassable terrain to deliver critical materials directly to the isolated fire points, and subsequently returns to rendezvous with the same truck at another synchronized node along the truck's ongoing route. This air–ground collaborative mechanism effectively bridges the gap between road accessibility limitations and the 'last-mile' delivery requirements.

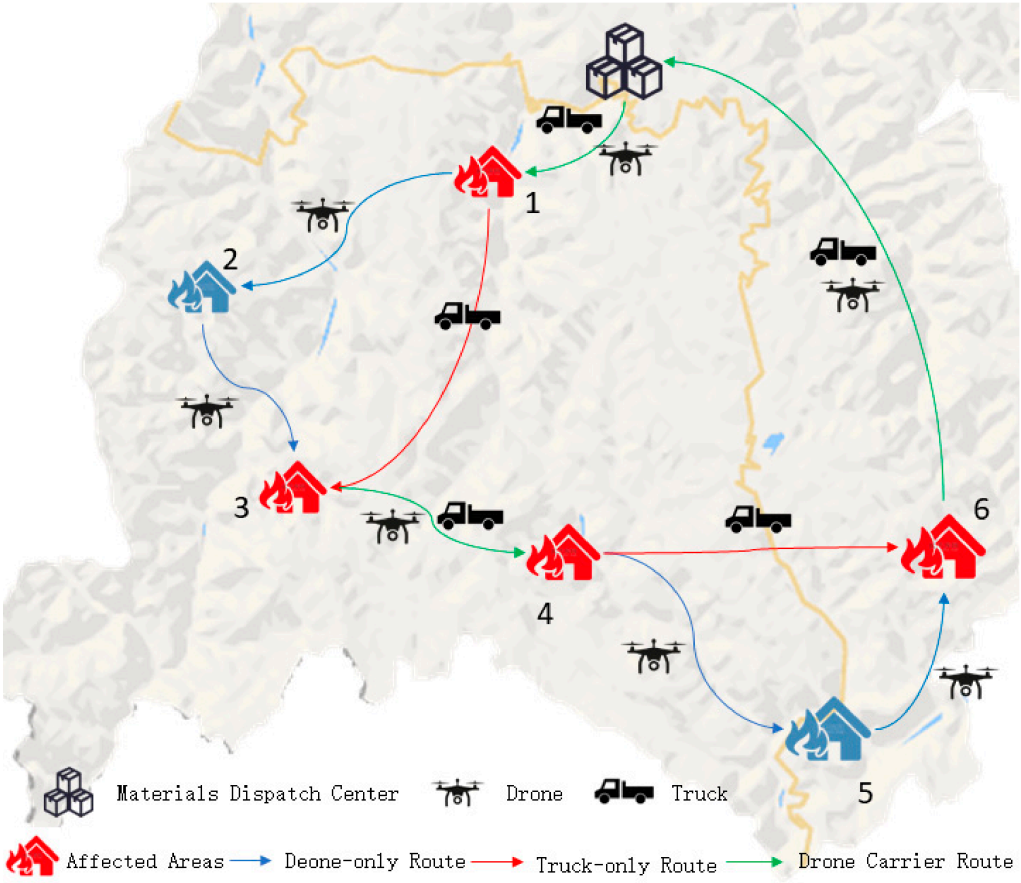


Figure 1. Illustrative routing map of the truck–UAV collaborative material dispatch process in the disaster-affected area.

3.2. Method Justification and the FACO-GA Framework

As a typical complex system, air–ground collaborative emergency dispatch under dynamic environments involves strong coupling among multiple influencing factors. Traditional static optimization methods treat decision variables as independent, making it difficult to accurately capture the dynamic constraints of a continuous disaster evolution.

In existing studies, single heuristic algorithms such as the Genetic Algorithm (GA) or Ant Colony Optimization (ACO) have been widely applied to routing problems. However, when faced with high-dimensional, multi-constrained, and multi-objective dynamic rescheduling scenarios, single algorithms exhibit significant limitations. GA possesses strong global exploration capabilities but lacks local search precision, often leading to premature convergence. Conversely, ACO excels at local refined searching and sequential routing but suffers from slow initial convergence and a tendency to fall into local optima.

To overcome these limitations, this study proposes a Fast Ant Colony Optimization-Genetic Algorithm (FACO-GA) integrated with a rolling-horizon optimization mechanism. By fusing the two approaches, the FACO-GA utilizes the Genetic Algorithm for global high-level decisions (e.g., vehicle–task assignment and multi-objective trade-offs) and employs the Ant Colony Algorithm for secondary localized refinement of specific flight and driving paths. The flowchart of the ant colony genetic algorithm is shown in Figure 2.

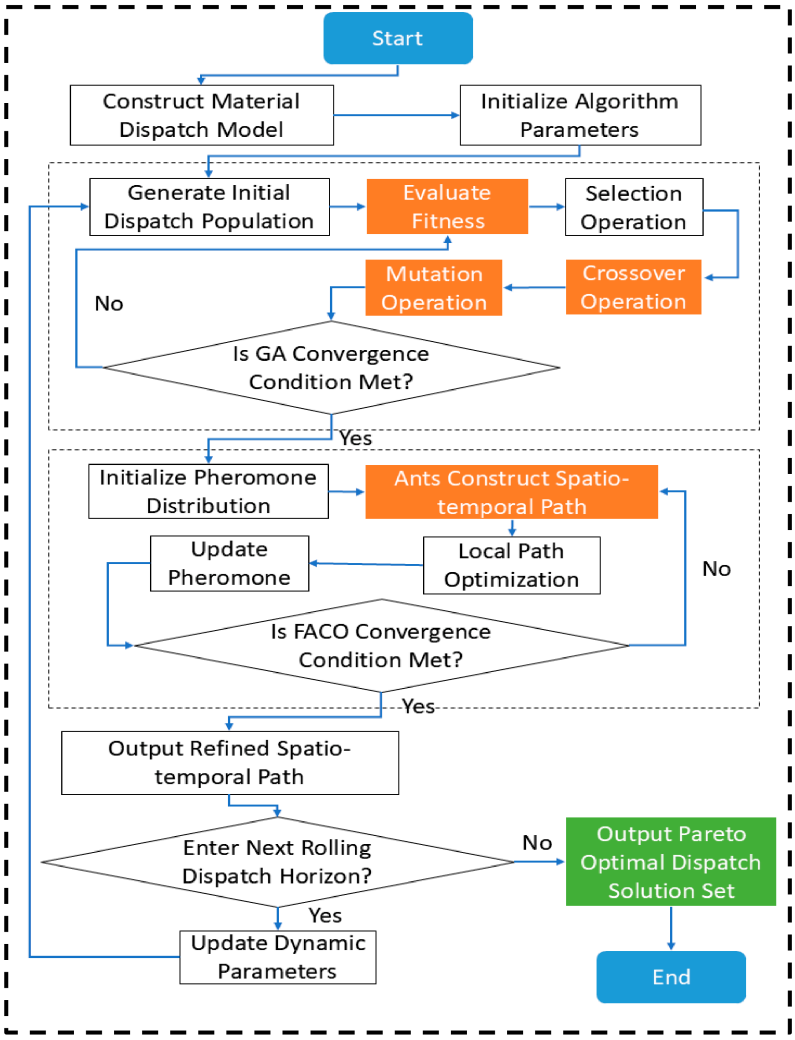


Figure 2. Flowchart of the proposed Fast Ant Colony-Genetic Algorithm (FACO-GA) with rolling-horizon optimization.

Specifically, the proposed FACO-GA effectively leverages the complementary strengths of both algorithms in two dimensions:

- **Global Decision-Making via GA**: The GA module is responsible for macro-level resource allocation and task assignment (e.g., determining the division of labor between trucks and UAVs). It achieves multi-objective trade-offs among response time, cost, and fairness through non-dominated sorting. In addition, its mutation mechanism maintains population diversity and prevents premature convergence in dynamic environments.
- **Local Refined Exploitation via ACO**: Operating within the initial framework generated by the GA, the ACO module executes specific path planning and sequence construction. Its pheromone-feedback mechanism enables deep local micro-adjustment under multiple constraints (e.g., endurance, payload, and safety intervals), making it highly efficient for rapid topology repair following sudden dynamic perturbations.

3.3. Mathematical Model Formulation

To accurately capture the dynamic trade-offs in emergency material dispatch and provide precise fitness-evaluation criteria for the FACO-GA, this study formulates the problem as a multi-objective mixed-integer linear programming (MOMILP) model. Instead of relying on a weighted-sum approach, the model establishes a Pareto optimization

framework to independently and simultaneously optimize three conflicting objectives: emergency response time, total operational cost, and rescue fairness.

3.3.1. Description of Symbols

To comprehensively represent the system state and decision-making process across spatial, temporal, resource, and behavioral dimensions, the parameters and variables used in the mathematical model are defined in Table 2.

Table 2. Description of sets, parameters, and variables used in the MOMILP model.

Category	Symbol	Meaning
Sets	V_T	Set of available trucks, indexed by v
	V_U	Set of available UAVs, indexed by u
	N	Set of all nodes in the network, $N = \{0\} \cup N_C \cup \{n+1\}$
	W	Set of dynamic scheduling time windows, indexed by w.
	N_C	Set of disaster-affected demand points, indexed by i, j, k
	N'	Set of truck-accessible nodes ($N' \subseteq N$)
Parameters	q_i	Initial material demand at affected point $i \in N_C$
	Q_T	Maximum payload capacity of trucks
	Q_U	Maximum payload capacity of UAVs
	e	Maximum endurance (flight time) of a UAV per sortie
	$d_{\max}$	Maximum flight distance of a UAV per sortie
	t_{ij}^T	Truck travel time from node i to j
	t_{ij}^U	UAV flight time from node i to j
	c_T	Unit operational cost per unit time for trucks
	c_U	Unit operational cost per unit time for UAVs
	g_i	Binary parameter: 1 if node i is truck-accessible; 0 if road is blocked
	M	A sufficiently large positive number
Variables	x_{ij}^v	Binary variable: 1 if truck v travels directly from node i to j; 0 otherwise
	y_{ikj}^u	Binary variable: 1 if UAV u takes off from ground node i, serves the disaster-affected node k, and lands at ground node j to reunite with its paired truck; 0 otherwise.
	s_i	Continuous non-negative variable: Actual quantity of materials supplied to point i
	T_{vw}^{end}	Continuous non-negative decision variable representing the final return time of truck v to the depot in window w.
	T_{uw}^{end}	Continuous non-negative decision variable representing the final return time of UAV u to the depot in window w.
	T_i^v	Continuous non-negative variable: Time at which truck v arrives at node i
	u_i^v	Auxiliary continuous variable for sub-tour elimination in routing

3.3.2. Mathematical Model

To accurately characterize the dynamic and time-varying features of complex high-altitude mountain rescue environments, we introduce the concept of a multi-period rolling horizon. Let $w \in W$ denote the current dynamic scheduling window. State parameters (such as road accessibility and material demand) are dynamically updated at the beginning of each window w. The multi-objective mixed-integer linear programming (MOMILP) model evaluated by the FACO-GA framework is formulated as follows:

1. Multi-Objective Functions

Based on the abstract's requirement to jointly optimize time, cost, and fairness, the objective functions are defined as:

- **Objective 1**: Minimize Maximum Emergency Response Time

This objective aims to minimize the maximum mission completion time among all dispatched vehicles within the current scheduling window w. $T_{v,w}^{end}$ and $T_{u,w}^{end}$ represent the final return times for truck v and UAV u in window w.

$$f_1 = \text{minmax}\left(\max_{v \in V_T} T_{v,w}^{end}, \max_{u \in V_U} T_{u,w}^{end}\right)$$

- **Objective 2**: Minimize Total Dispatch Cost

This objective calculates the cumulative comprehensive transportation cost across all scheduling windows, integrating the ground travel costs of trucks and the aerial flight costs of UAVs. c_T and c_U are the unit time operational costs for trucks and UAVs, respectively.

$$f_2 = \min\left(\sum_{v \in V_T}\sum_{i \in N'}\sum_{j \in N'} c_T \cdot t_{ij}^T \cdot x_{ij}^v + \sum_{u \in V_U}\sum_{i \in N'}\sum_{k \in N_C}\sum_{j \in N'} c_U \cdot \left(t_{ik}^U + t_{kj}^U\right) \cdot y_{ikj}^u\right)$$

- **Objective 3**: Maximize Rescue Fairness

To prevent extreme disparities in resource distribution, this objective strictly quantifies fairness by minimizing the maximum difference in the unmet demand ratio among all affected disaster points. q_i^w represents the dynamic material demand of node i in window w, and s_i^w is the actual quantity supplied during that window.

$$f_3 = \min\left[\max_{i \in N_C}\left(\frac{q_i^w - s_i^w}{q_i^w}\right) - \min_{j \in N_C}\left(\frac{q_j^w - s_j^w}{q_j^w}\right)\right]$$

2. Network Routing and Flow Balance Constraints

- **Constraint 1**: Truck Departure Constraint

This ensures that in any scheduling window w, all actively dispatched trucks v should originate their routes from the central material distribution center (depot 0).

$$\sum_{j \in N'} x_{0j}^{vw} = 1, \forall \text{v} \in V_T, \forall w \in W$$

- **Constraint 2**: Truck Return Constraint

This requires that all trucks v should successfully return to the central dispatch center (represented as depot $n+1$) upon completing their tasks in window w.

$$\sum_{i \in N'} x_{i,n+1}^{vw} = 1, \forall v \in V_T, \forall w \in W$$

- **Constraint 3**: Physical Flow Balance Constraint

This guarantees the physical continuity of the ground routes. It ensures that if truck v enters a specific node j during window w, it should identically depart from that node j to continue its journey.

$$\sum_{i \in N'} x_{ij}^{vw} = \sum_{k \in N'} x_{jk}^{vw}, \forall j \in N', \forall v \in V_T, \forall w \in W$$

- **Constraint 4**: Sub-tour (Visit Sequence) Elimination Constraint

This prevents the algorithm from generating closed-loop invalid routes that fail to connect back to the main depot. u_i^v is an auxiliary continuous variable representing the sequential visitation order of node i by truck v.

$$u_i^v - u_j^v + \left|N_C\right| \cdot x_{ij}^{vw} \leq \left|N_C\right| - 1, \forall i, j \in N_C, \forall v \in V_T, \forall w \in W$$

3. Task Assignment and Dynamic Environmental Constraints

- **Constraint 5**: Single Service/Comprehensive Coverage Constraint

This ensures that across the multi-period scheduling timeline W, every identified disaster demand point j is served efficiently, avoiding duplicated or wasted dispatches.

$$\sum_{w \in W} \left(\sum_{v \in V_T} \sum_{i \in N'} x_{ij}^{vw} + \sum_{u \in V_U} \sum_{i \in N'} \sum_{k \in N_C} y_{ikj}^{uw} \right) \geq 1, \forall j \in N_C$$

- **Constraint 6**: Dynamic Supply and Demand Bounding Constraint

The actual material supply s_i^w to an affected point i should not exceed its dynamically updated demand threshold q_i^w for that specific window w.

$$0 \leq s_i^w \leq q_i^w, \forall i \in N_C, \forall w \in W$$

- **Constraint 7**: Inaccessible Point Constraint

This embeds environmental uncertainty. We introduce g_i^w, a time-varying binary parameter that equals 1 if node i is truck-accessible and 0 if the road is blocked in window w. If $g_i^w = 0$, trucks cannot travel to/from it, meaning the node should only be served via UAV airdrops.

$$x_{ij}^{vw} \leq \min\{g_i^w, g_j^w\}, \forall i, j \in N', \forall v \in V_T, \forall w \in W$$

4. Capacity Constraints

- **Constraint 8**: Truck Payload Capacity Constraint

This restricts the total weight of materials offloaded by truck v across all its designated stops in window w from exceeding its maximum structural payload capacity Q_T.

$$\sum_{j \in N_C} s_j^w \cdot x_{ij}^{vw} \leq Q_T, \forall v \in V_T, \forall w \in W$$

- **Constraint 9**: UAV Payload Capacity Constraint

This limits the total materials airdropped by UAV u during a single sortie (flight mission serving node k) to its maximum payload limit Q_U.

$$\sum_{k \in N_C} s_k^w \cdot y_{ikj}^{uw} \leq Q_U, \forall u \in V_U, \forall w \in W$$

5. Air–Ground Spatiotemporal Collaboration Constraints

- **Constraint 10**: UAV Takeoff/Landing and Task Quantity Constraint

The core logic for collaborative relay. It requires that UAV u should only initiate a flight from node i, serve k, and land at node j, if and only if its exclusively paired truck v is actively traveling the ground segment between node i and j in window w.

$$y_{ikj}^{uw} \leq x_{ij}^{vw}, \forall i, j \in N', \forall k \in N_C, \forall u \in V_U, \forall v \in V_T, \forall w \in W$$

- **Constraint 11**: UAV Flight Endurance Constraint

This ensures that the total continuous flight time of UAV u per sortie (traveling $i \to k$ and $k \to j$) is less than or equal to its maximum battery endurance time e.

$$\left(t_{ik}^{U} + t_{kj}^{U}\right) \cdot y_{ikj}^{uw} \le e, \forall i, j \in N', \forall k \in N_C, \forall u \in V_U, \forall w \in W$$

- **Constraint 12**: UAV Maximum Flight Distance Constraint

This ensures the spatial linear flight trajectory of the UAV does not exceed its maximum structurally permitted flight distance $d_{\max}$.

$$\left(d_{ik} + d_{kj}\right) \cdot y_{ikj}^{uw} \le d_{\max}, \forall i, j \in N', \forall k \in N_C, \forall u \in V_U, \forall w \in W$$

- **Constraint 13**: Air–Ground Time Synchronization Constraint

To align the mathematical model with real-world operational constraints, t^{load} is introduced to denote the material loading and unloading duration at ground nodes. Furthermore, t^{safe} represents the temporal buffer required for UAV takeoff and landing safety intervals. This ensures strict chronological logic between the truck and UAV operations.

$$T_i^v + t_{ij}^T + t^{load} + \left(t_{ik}^{U} + t_{kj}^{U} + 2 \cdot t^{safe}\right) \cdot y_{ikj}^{uw} \le T_j^v + M\left(1 - x_{ij}^{vw}\right)$$

6. Variable Domain Constraints

- **Constraint 14**: 0–1 Decision and Non-negativity Constraints

This specifies the mathematical bounds of the variables, conforming to actual physical meanings.

$$x_{ij}^{vw}, y_{ikj}^{uw} \in \{0, 1\}$$

$$T_{i,w}^v \ge 0, s_i^w \ge 0, u_i^v \ge 0$$

These objective functions and constraints jointly enforce route continuity, single-service assignment, payload limits, UAV endurance and range, and spatiotemporal synchronization between trucks and UAVs.

Note on Model Complexity and Non-linearity: Several objectives and constraints formulated above exhibit non-linear characteristics, which significantly increase the problem's complexity. Specifically, the min-max structure in Objective 3 (f_3) is inherently non-linear. Furthermore, Constraints 8, 9, 11, and 13 involve combinations of continuous and binary variables (e.g., multiplication of time/payload variables with routing binary variables). In this study, the non-linear time synchronization in Constraint 13 is linearized using the 'Big M' method, while the remaining non-linearities in the objective functions and payload evaluations are directly handled by the fitness evaluation mechanism of the proposed FACO-GA heuristic, circumventing the need for complex algebraic transformations.

3.4. Network Definition and Operational Constraints

The air–ground collaborative dispatch process is defined within a comprehensive transportation network that includes a central material distribution center (depot) and multiple affected areas. Each affected area has a specific relief resource demand that must be fulfilled before a strict delivery deadline.

Delivery operations are executed by a fleet of dedicated truck–UAV pairs. Each truck acts as both a ground main-line transport vehicle and a mobile launching and recovery platform for its exclusively paired UAV. A UAV can launch from its associated truck at a specific location, independently deliver resources to one or more affected areas, and

rendezvous with the same truck at another location along its route. To ensure operational consistency, a UAV is strictly prohibited from launching from or returning to a truck other than its designated pair.

Trucks and UAVs differ significantly in payload capacity and travel efficiency. Trucks possess a substantially larger payload capacity than UAVs. Furthermore, since UAVs perform point-to-point linear flights while trucks must navigate the surface road network, the UAV flight time between any two locations is generally shorter than the corresponding truck travel time. Additionally, aerial operations are strictly constrained by the UAV's maximum battery life, which dictates the maximum continuous flight duration per sortie.

To provide a clear understanding of the systemic interaction between different functional nodes, the operational workflow of the air–ground collaborative network is visualized. As shown in Figure 3, the model characterizes the movement of materials from the central depot through various transit points, where trucks serve as mobile bases for UAV launching and recovery to reach specific affected areas.

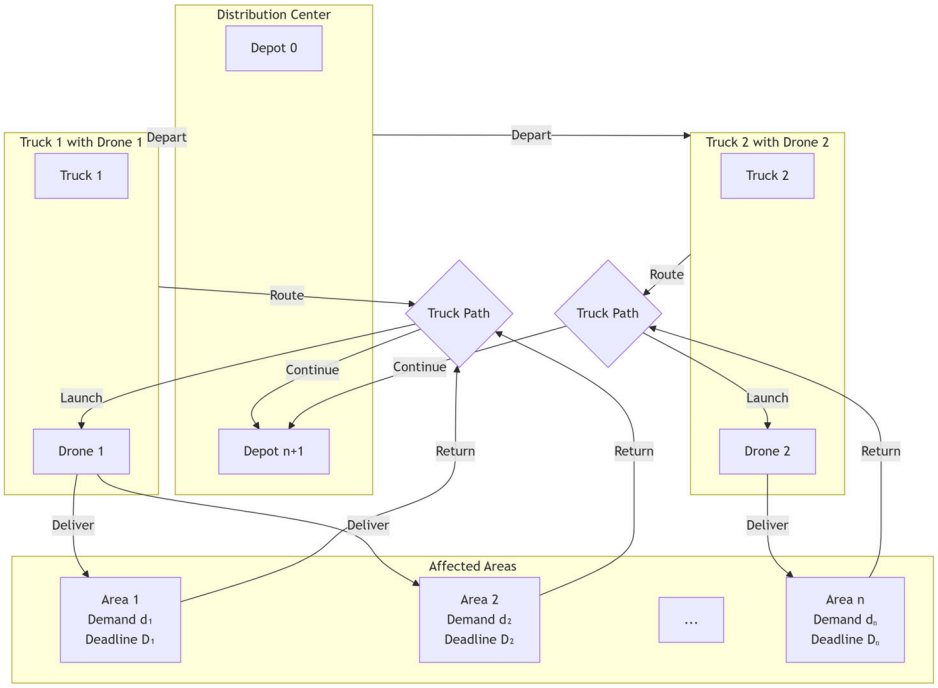


Figure 3. Logical architecture and operational flow of the truck–UAV collaborative dispatching network.

The problem under consideration is defined on a complete directed graph G = (N, A), where N = {0, n + 1}∪C is the set of nodes. This includes depot nodes 0 and n + 1, both of which represent the central material dispatch center, and a set of affected nodes C = {1, . . . , k}, where each node corresponds to a disaster-affected area. Each affected area has a specific relief resource demand and a strict deadline. The relief resources must be delivered to the area before this deadline to ensure that the victims receive timely assistance.

The transportation of rescue resources from the dispatch center to the affected areas is collaboratively executed by homogeneous rescue trucks and UAVs initially located at the depot, with each truck equipped with a dedicated UAV. Each truck can simultaneously perform its own ground transportation operations and act as an intermediate mobile depot. Furthermore, each UAV can independently execute its own aerial transportation operations to the affected areas. Specifically, a UAV launches from its associated truck at a certain node, delivers the relief resources to one or more affected areas before their respective deadlines, and subsequently returns to the truck at another node along the truck's planned

route. Since each UAV is exclusively paired with a specific truck, it is strictly prohibited from launching from or returning to a different truck.

Let K = {1, …, k} be the set of available truck–UAV pairs. Trucks and UAVs differ significantly in payload capacity, travel speed, and travel routes. The payload capacities of the truck and its paired UAV are denoted as Q_H and Q_U respectively. Since the truck acts as the mobile base for its paired UAV in collaborative tasks, it must hold a larger capacity, such that $Q_U < Q_H$. Note that this strict payload constraint applies exclusively to the paired truck–UAV synergy operations (e.g., Trucks and HY100), whereas long-range heavy UAVs fly independently directly from the depot. We assume that UAVs can fly in a straight line from one location to another, taking advantage of the three-dimensional airspace, while trucks are strictly constrained by the surface road network. Therefore, the flight time for a UAV traversing each arc is generally shorter than the corresponding travel time for a truck. Without loss of generality, we assume that both the truck travel times and the UAV flight times satisfy the triangle inequality. Finally, the maximum battery life of each UAV is denoted as E, which strictly dictates its maximum continuous flight duration per sortie.

Based on these defined network and operational constraints, the dispatch process dynamically evolves across multiple phases to prioritize high-demand areas while ensuring resource coverage. Figure 4 illustrates the conceptual evolution of these scheduling plans, demonstrating how trucks and drones collaborate and split routes over successive scheduling horizons.

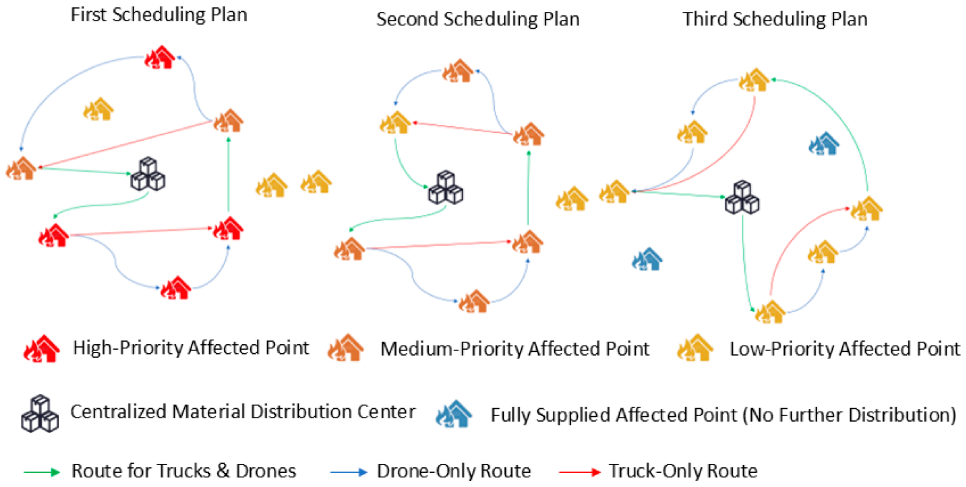


Figure 4. Conceptual illustration of the dynamic air–ground collaborative scheduling phases and route splitting.

3.5. Rolling Horizon Optimization Mechanism

To effectively manage the dynamic time-varying parameters (e.g., rapid fire spread, sudden road blockages) described in the network constraints, the proposed FACO-GA incorporates a rolling horizon mechanism. Instead of attempting a single global optimization that may quickly become obsolete, the continuous rescue process is discretized into sequential decision windows. The mechanism operates through three core steps:

- **State Update & Trigger:** When the system receives real-time environmental perturbation data that alters network topology or node availability, the re-optimization process is dynamically triggered.
- **Local Topology Repair**: The algorithm freezes the already executed tasks and dynamically maps the unfulfilled demands and affected nodes into a new, localized temporal window.

- **Re-optimization and Inheritance:** The ACO module then utilizes the historically accumulated pheromones from the previous horizon. This allows the algorithm to rapidly reconstruct localized routing paths and bypass blind global recalculations, maintaining high adaptability to new constraints.

4. Experimental Simulation and Result Analysis

4.1. Construction of the Simulation Scenario

To comprehensively validate the effectiveness and superiority of the proposed FACO-GA framework under dynamic time-varying characteristics, a simulation experiment was designed based on real-world geographic and demographic data. All multi-objective scheduling simulation experiments in this paper were conducted on a computer equipped with an Intel Core i7-12700H processor and 16 GB of RAM, running Windows 11. The algorithm code was developed using MATLAB R2024b, while terrain modeling and result visualization were performed on the same platform.

The experiment is contextualized within the high-plateau mountainous terrain of Muli County, Liangshan Prefecture, Sichuan Province. This region exhibits an average altitude exceeding 3100 m, with extreme vertical drops between river valleys and mountain ridges. To accurately reflect this operational constraint, a three-dimensional terrain grid was constructed using SRTM elevation data. To accurately reflect this operational constraint, a three-dimensional terrain grid was constructed using Shuttle Radar Topography Mission (SRTM) elevation data, as shown in Figure 5. This model highlights the extreme vertical drops that dictate the physical constraints of ground transport and the spatial requirements for UAV flight paths.

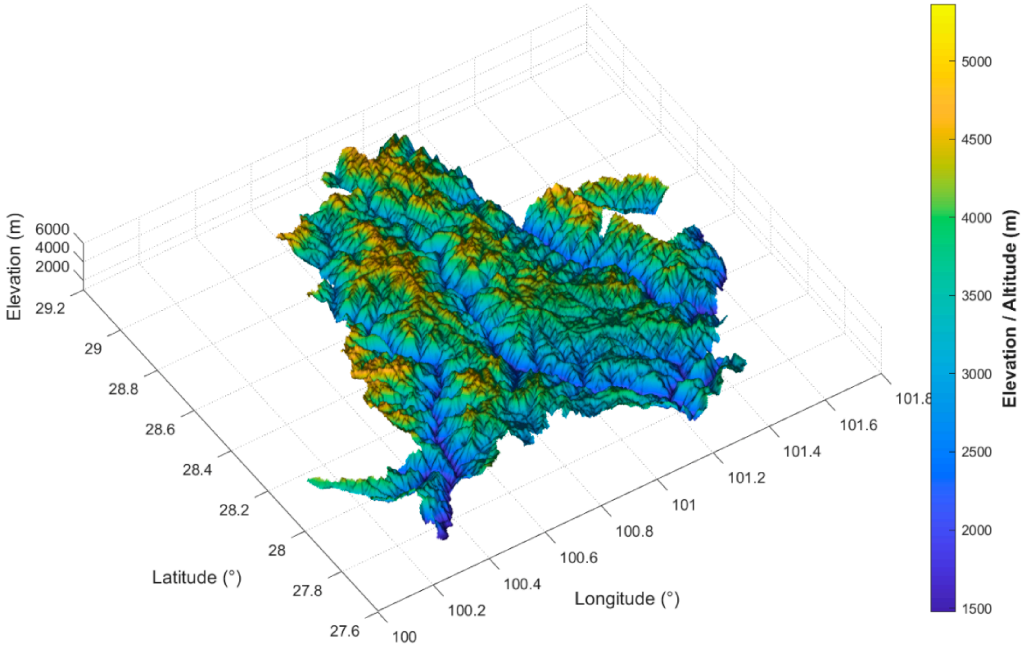


Figure 5. Three-dimensional terrain elevation model of the Muli County study area.

In practical material dispatch, disaster points often correlate with human activity. Therefore, recent population data from the Geographic National Monitoring Cloud Platform was processed to generate a population heat map of the region.

Based on the population density and terrain characteristics, spatial clustering algorithms were applied to extract 21 representative affected points within the research area. Figure 6 displays the population density heat map and the spatial distribution of these selected affected points, reflecting the correlation between demographic density and ini-

tial material demand, which varies between 150 kg and 400 kg and yields a total system demand of approximately 6450 kg.

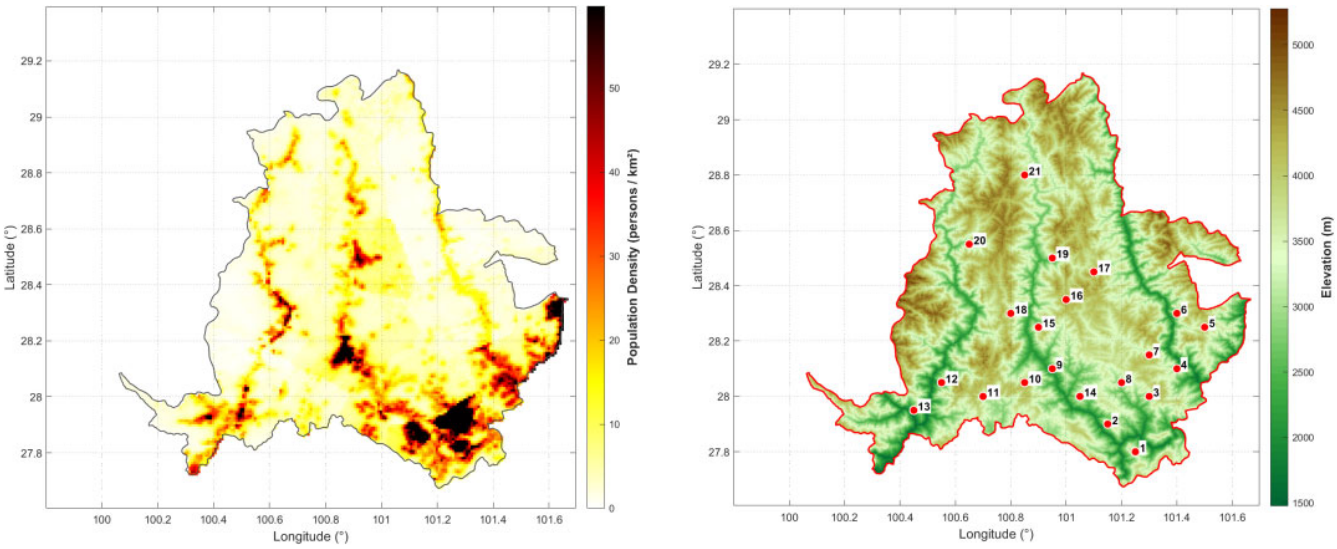


Figure 6. Population density heat map and spatial distribution of the 21 selected affected points.

4.2. Fleet Capacity and Configuration

Suppose that 21 locations in Muli County simultaneously experience forest fires, designated as fire points 1, 2, 3, . . . , 21, respectively; both trucks and UAVs utilize a single centralized material dispatch center as their supply source, and this centralized material dispatch center (Base) is strategically located near the Muli County transportation hub, an area characterized by relatively flat terrain and a dense traffic network. Considering the road damage caused by the complex terrain of Muli County, this experiment adopts a heterogeneous fleet air–ground collaborative model. The system is configured with 8 trucks, 4 Twin-tailed Scorpion D heavy-duty UAVs, and 4 HY100 medium-duty UAVs, all departing from the same centralized material dispatch center. The performance parameters of the fleet are presented in Table 3.

Table 3. Performance Parameters of the Transport System.

Vehicle Type	Speed (km/h)	Maximum Flight Distance (km)	Maximum Payload (kg)	Maximum Endurance (h)
Truck	40	-	2000	-
Twin-tailed Scorpion D	300	6000	2800	35
HY100	330	1800	500	10.6

4.3. Generation Mechanism of Node Material Demand and Environmental Parameters

To ensure the physical feasibility and computational rigor of the scheduling model, this experiment assumes that the Central Material Dispatch Center (Base) has sufficient initial emergency reserves, with a total capacity set at 10,000 kg. For the 21 extracted disaster points (P1–P21), their initial material demand *Di* is not randomly generated blindly but calculated based on real geospatial data. The experiment imports the 2020 1 km resolution population density raster data of Muli County provided by WorldPop. The algorithm extracts the population density value at each disaster point's coordinates as a weight factor. Combined with a uniform pseudorandom function, the basic demand for each point is generated within the range of 150 kg to 400 kg. The cumulative system material demand is 6450 kg. The dispatched materials primarily consist of critical consumables (e.g.,

bottled water, combat rations, and emergency medical kits) and basic non-consumables (e.g., fire-retardant blankets). Because consumables are continuously depleted by frontline responders, their demand is highly dynamic. To closely reflect reality, the initial material demand D_i is not randomly generated blindly; it is quantitatively derived by weighting the actual 2020 1 km resolution population density raster data of Muli County (provided by WorldPop) against initial fire intensity reports. The specific demand distribution is detailed in Table 4.

Table 4. Presumed Material Demand for Disaster Points.

Point ID	Demand (kg)
P1	350
P2	300
P3	280
P4	250
P5	200
P6	310
P7	390
P8	320
P9	380
P10	350
P11	290
P12	260
P13	330
P14	370
P15	400
P16	360
P17	340
P18	310
P19	280
P20	180
P21	200

With the simulation scenario and fleet capacity established, the algorithm parameters must be properly configured to ensure optimal performance. To balance global exploration and local exploitation capabilities, the maximum number of iterations for the FACO-GA was set to 200. In the genetic operations, to fully explore the high-dimensional solution space and prevent premature convergence, the crossover and mutation probabilities were set to 0.8 and 0.2, respectively. For the ant colony optimization phase, the pheromone evaporation factor was set to 0.1 to maintain a reasonable balance between historical information accumulation and new path exploration. The iteration termination condition for the FACO-GA is met when the maximum number of iterations (200) is reached, or when the relative change in the Pareto front hypervolume remains less than $\mathbf{10^{-4}}$ for 20 consecutive iterations, indicating algorithmic convergence.

4.4. Analysis of the Collaborative Dispatch Scheme

Operating under the capacity and endurance constraints of a heterogeneous fleet (8 trucks, 4 heavy-duty UAVs, and 4 medium-duty UAVs), the FACO-GA intelligently segmented the rescue operations into three dynamic scheduling periods based on population density and urgency.

The resulting spatial routing scheme successfully decoupled the geographical limitations of ground transport from the payload limitations of aerial transport, achieving seamless relay operations across cliff-interrupted road networks. The specific routing

trajectories generated by the algorithm are presented in Figure 7, detailing the distinct operational paths taken by trucks, mid-range UAVs, and long-range heavy-duty UAVs.

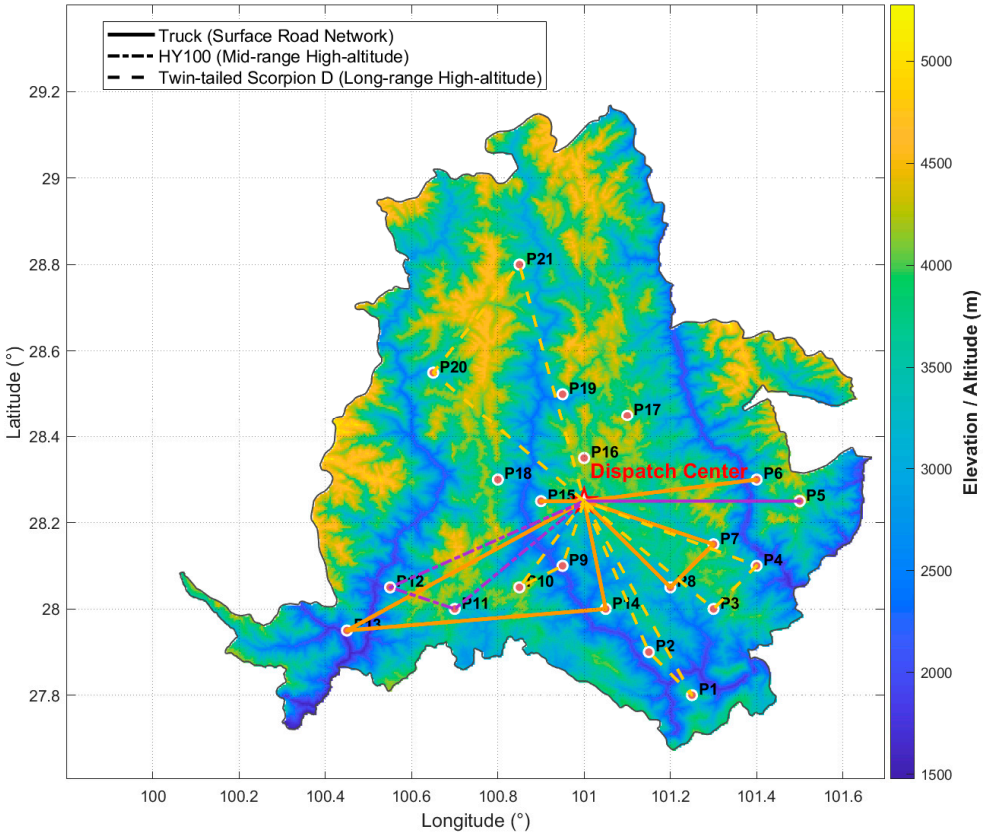


Figure 7. Spatial routing trajectories of the heterogeneous fleet generated by the FACO-GA.

Based on population density and demand urgency, the hybrid algorithm effectively segmented the dispatch scheme into three dynamically evolving phases:

1. **Cycle 1: Prioritizing the Extremely Densely Populated Southeastern Deep Valleys and Suburban High-Demand Areas**

Since the FACO-GA outputs a set of non-dominated Pareto-optimal solutions, selecting the final execution scheme requires balancing the three conflicting objectives. In this study, the Technique for Order of Preference by Similarity to Ideal Solution (TOPSIS) with equal weights assigned to response time, cost, and fairness is employed to select the final compromise solution from the Pareto set for practical command operations. In the initial iteration, the hybrid algorithm prioritized the most densely populated Yalong River valley zone (P1–P8) and suburban points (P15), concentrating the highly efficient transport capacities of heavy UAVs and ground trucks. The details are shown in Table 5.

Table 5. Scheduling Plan for Cycle 1.

Eqpt. ID	Vehicle/UAV Type	Transport Mode	Target Points	Detailed Routing Path
S1	Twin-tailed Scorpion D	UAV Direct Flight	P1, P2	Base → P1 → P2 → Base
S2	Twin-tailed Scorpion D	UAV Direct Flight	P3, P4	Base → P3 → P4 → Base
H1	HY100	UAV Direct Flight	P5	Base → P5 → Base
T1	Truck	Truck Only	P6	Base → P6 → Base
T2	Truck	Truck Only	P15	Base → P15 → Base
T3 + H2	Truck + HY100	Truck–UAV Synergy	P7, P8	T3 offloads 390 kg at P7; H2 takes off from P7 with 320 kg to airdrop at P8

2. **Cycle 2: Focusing on Medium-Density Southern Rivers and Mid-Distance Complex Valleys**

As the demand in extremely severely afflicted areas was alleviated, the algorithm shifted its focus southward (P9–P14, P16–P17). Due to the complex terrain and severely damaged roads in this area, the algorithm significantly increased the utilization ratio of the truck–UAV collaborative mode. The details are shown in Table 6.

Table 6. Scheduling Plan for Cycle 2.

Eqpt. ID	Vehicle/UAV Type	Transport Mode	Target Points	Detailed Routing Path
S3	Twin-tailed Scorpion D	UAV Direct Flight	P9, P10	Base → P9 → P10 → Base
H3	HY100	UAV Direct Flight	P11, P12	Base → P11 → P12 → Base
T4	Truck	Truck Only	P16	Base → P16 → Base
T5	Truck	Truck Only	P17	Base → P17 → Base
T6 + H4	Truck + HY100	Truck–UAV Synergy	P13, P14	T6 drives to P13 and offloads 330 kg; H4 takes off from P13 with 370 kg, crossing a cliff to P14

3. **Cycle 3: Sweeping Extremely Remote High-Altitude Islands and Peripheries**

In the final scheduling phase, the algorithm detached from conventional road network constraints. For the extremely high-altitude pastoral areas in the northwest with sparse populations (P20, P21), long-endurance UAVs were directly assigned for aerial penetration, while the remaining trucks completed sweeping deliveries for peripheral nodes. The details are shown in Table 7.

Table 7. Scheduling Plan for Cycle 3.

Eqpt. ID	Vehicle/UAV Type	Transport Mode	Target Points	Detailed Routing Path
S4	Twin-tailed Scorpion D	UAV Direct Flight	P20, P21	Base → P20 → P21 → Base
T7	Truck	Truck Only	P18	Base → P18 → Base
T8	Truck	Truck Only	P19	Base → P19 → Base

5. In-Depth Analysis of Dynamic Rescheduling Mechanisms

While Section 3 analyzed the initial static dispatch scheme, real-world high-plateau wildfire environments are highly volatile. To evaluate the robustness of the FACO-GA in real-time crisis scenarios (e.g., sudden wind shifts, secondary road blockages), dynamic perturbations ranging from levels 1 to 10 were introduced into the simulation. This requires the algorithm to possess rapid and stable rescheduling capabilities, rather than merely generating static optimal solutions.

5.1. Parameterization of Dynamic Perturbations and Rolling Horizon Mechanism

To transform the conceptual verification into a reproducible experimental framework, this section defines the mathematical mapping of environmental disturbances and the operational parameters of the rolling horizon mechanism.

5.1.1. Mapping Environmental Disturbances to Network Parameters

The dynamic perturbations (Level 1–10) are defined as a multi-factor stochastic coupling of wildfire spread, road infrastructure degradation, and meteorological fluctuations. Each level $\mathbf{L} \in \{\mathbf{1}, \ldots, \mathbf{10}\}$ linearly scales the intensity of three primary disturbance vectors:

1. Meteorological Drag (M_L): Affects UAV travel time. High-altitude wind shifts cause a speed reduction of.

2. Road Degradation (R_L): Affects truck travel time. Fire-induced smoke and debris reduce ground velocity by, a "Critical Blockage" probability is introduced for random edges in the ground network.
3. Demand Surge (D_L): Wildfires are inherently dynamic disasters. Consequently, the material demand q_i^w does not remain static but evolves continuously across scheduling windows due to fire spread and localized resource depletion. In the simulation, as the fire perimeter expands, new frontline rescue personnel are deployed, and secondary evacuations occur. This dynamic behavior is explicitly modeled using a time-varying demand update function:

$$q_i^{w+1} = \mathbf{max}(0, q_i^w - s_i^w) \times \mathbf{D_L} + \Delta q_{new}$$

where $\mathbf{D_L}$ is the demand surge factor driven by the spreading fire, and $\boldsymbol{\Delta q_{new}}$ represents newly generated demand. The FACO-GA's rolling horizon mechanism responds to these dynamic shifts by adaptively reallocating trucks and UAVs in each subsequent time window, ensuring that newly emerged demands are promptly met.

5.1.2. Rolling Horizon Configuration

The rolling horizon mechanism discretizes the continuous rescue mission into sequential decision intervals to manage the evolving environment:

Window Length ($\mathbf{\Delta T}$): Set to 30 min. This length is strategically configured based on the typical response-cycle requirements of firefighting logistics and the average fire-spread velocity in the Muli region, ensuring that the model updates at a rate faster than the disaster's environmental evolution.

Trigger Condition ($\mathbf{\Gamma}$): Re-optimization is triggered if (a) a ground route blockage occurs or (b) the cumulative deviation in arrival times exceeds 15% of the window length.

Task Freezing Rule: All materials already offloaded and vehicles currently in transit to a node are "locked" and cannot be reassigned during the current rescheduling cycle.

Pheromone Inheritance: The ACO module retains 60% of the pheromone density from the previous window to accelerate local topology repair, while 40% is evaporated to allow for new path exploration.

5.1.3. Experimental Reliability and Reproducibility

To ensure the statistical significance of the results (Figure 8) and eliminate accidental bias:

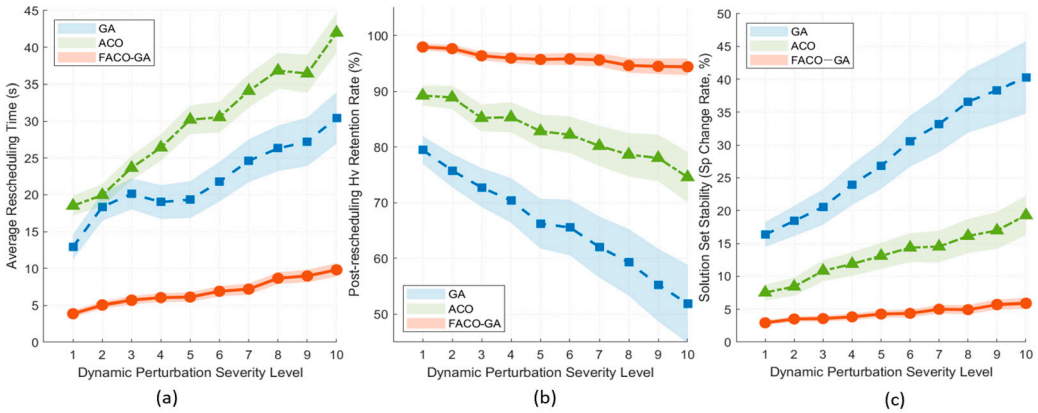


Figure 8. Multi-objective performance comparison chart: (**a**) Average rescheduling time; (**b**) Hv retention rate; (**c**) Sp change rate.

Repetitions for Statistical Significance: To eliminate the contingency of a single experimental outcome and guarantee reproducibility, each perturbation level was simulated for

50 independent runs. The results presented in subsequent sections represent the robust average performance across these iterations. Stochasticity: A fixed random seed was utilized in MATLAB to ensure that the spatial distribution of random blockages and demand surges is consistent across algorithm comparisons (GA vs. ACO vs. FACO-GA).

Confidence Intervals: Results in Table 8 are presented to reflect the algorithm's performance boundaries.

Table 8. Parameterized Definition of Dynamic Perturbation Levels.

Perturbation Level (L)	UAV Speed Reduction	Truck Speed Reduction	Demand Surge Factor	Route Blockage Prob.
Level 1–3 (Minor)	12–16%	18–24%	1.05–1.15	0%
Level 4–6 (Moderate)	18–22%	27–33%	1.20–1.30	0%
Level 7–10 (Severe)	24–30%	36–45%	1.35–1.50	10–40%

5.2. Multi-Objective Performance Comparison of Rescheduling Under Dynamic Time-Varying Conditions

Before delving into the detailed evolutionary trends across different perturbation levels, Table 9 presents a quantitative summary of the core multi-objective performance metrics—average dynamic rescheduling time, post-rescheduling Hv retention rate, and Sp change rate—for the ACO, GA, and FACO-GA algorithms. This statistical overview highlights the overall robustness and convergence characteristics of the proposed hybrid approach compared to traditional standalone methods in handling dynamic environmental shifts.

Table 9. Comprehensive multi-objective performance comparison of algorithms under dynamic time-varying environments.

Algorithm	Average Dynamic Rescheduling Time (s)	Post-Rescheduling Hv Retention Rate (%)	Solution Set Stability (Sp Change Rate, %)
ACO	30.25 ± 7.18	83.75 ± 4.31	$+12.60 \pm 3.45$
GA	21.90 ± 5.17	67.40 ± 9.19	$+27.40 \pm 8.04$
FACO-GA	6.80 ± 1.72	96.30 ± 1.15	$+4.15 \pm 0.86$

To micro-analyze the anti-interference boundaries of each algorithm regarding response timeliness, solution quality, and rescue fairness under different disturbance levels, the dynamic rescheduling performance evolution trends are plotted. Figure 8 visually compares the average rescheduling time, Hypervolume (Hv) retention rate, and Spacing (Sp) change rate across the three algorithms.

From the perspective of algorithmic structure and multi-objective performance, the proposed FACO-GA demonstrates significant systemic advantages over traditional standalone algorithms across three core dimensions:

- **Computational Efficiency and Dimension Management** (Average Rescheduling Time): As shown in Figure 8a, as the intensity of dynamic disturbances increases, traditional algorithms like the Genetic Algorithm (GA) and Ant Colony Optimization (ACO) experience a steep, near-linear increase in computation time. This is primarily because standalone algorithms lack effective local memory inheritance mechanisms, forcing them into inefficient global recalculations that trigger dimensional explosions. In contrast, the FACO-GA integrates a rolling horizon and local repair mechanism. This structural approach enables the algorithm to precisely identify and repair localized

nodes affected by disturbances without blind global recalculation, compressing the extreme average response time to 6.80 s (remaining under 10 s even at Level 10 severity), thereby satisfying the strict real-time requirements of emergency command systems.

- **Solution Quality and Structural Retention** (Hypervolume Retention Rate): As shown in Figure 8b, the Hypervolume (Hv) metric reflects the comprehensive quality of the Pareto front in multi-objective optimization. Under severe environmental disruptions, the GA exhibits extreme vulnerability, with its Hv retention dropping precipitously below 60%. This indicates a catastrophic loss of elite genetic information, leading to degraded scheduling schemes. Conversely, the FACO-GA maintains a robust Hv retention rate of 96.30%. This finding indicates that the hybrid mechanism successfully preserves critical structural information from previous iterations, ensuring that the newly generated routing schemes remain highly proximal to the global Pareto-optimal front, thus perfectly balancing rescue efficiency and operational costs.
- **Systemic Stability and Rescue Fairness** (Spacing Change Rate): As shown in Figure 8c, in emergency logistics, the Spacing (Sp) metric directly maps to the fairness and stability of global resource distribution. Under medium-to-high disturbances, traditional algorithms exhibit Sp variations exceeding 15% to 35%. From a practical decision-making standpoint, this means traditional methods completely disrupt the global distribution rhythm to compensate for localized disruptions, resulting in polarized and highly unfair resource allocation. By contrast, the FACO-GA strictly controls the Sp variation within a tight 4.15% margin. This proves that the algorithm can smoothly reallocate heterogeneous transport capacity (trucks and UAVs) to disrupted nodes while preserving the operational rhythm of unaffected areas, maximizing systemic rescue fairness.

5.3. Algorithm Robustness and Variance Boundary Analysis

Beyond the average performance metrics, the stability of an emergency dispatch algorithm under random environmental noise is a critical indicator of its practical viability. In Figure 8, the shaded bands surrounding the primary trend lines represent the variance boundaries (confidence intervals) of the algorithmic performance across multiple simulation runs with stochastic perturbations.

- **Vulnerability of Traditional Algorithms to Stochasticity:** As the dynamic perturbation severity increases from Level 1 to 10, the shaded variance bands for both the Genetic Algorithm (GA) and Ant Colony Optimization (ACO) exhibit a distinct "trumpet-shaped" expansion. This severe divergence indicates that traditional standalone algorithms are highly sensitive to random environmental noise. Under strong disturbances, their search processes become chaotic, leading to extreme fluctuations in rescheduling time and solution quality. The wide variance bounds imply a high risk of catastrophic scheduling failure in real-world crisis management.
- **High Robustness of the FACO-GA Framework:** In stark contrast, the variance boundaries (red shaded areas) of the proposed FACO-GA remain exceptionally tight and narrow across all ten severity levels. This mathematically demonstrates the superiority of the rolling horizon and local repair mechanisms. Instead of blindly restarting the global search, the FACO-GA effectively absorbs localized stochastic shocks and inherits historical pheromone data. Consequently, it not only guarantees a highly optimal average performance but also ensures strict upper and lower execution bounds, providing a highly predictable and robust decision-making tool for emergency commanders.

In conclusion, the advantage of the proposed FACO-GA in dynamic, multi-factor-coupled scenarios does not solely rely on the extreme optimization of a single static metric.

Instead, its superiority lies in its systemic spatial decoupling, its resistance to computational dimension surges, and its highly adaptive local repair capabilities.

5.4. Component Contribution and Parameter Sensitivity Analysis

To stringently evaluate the independent contributions of the core modules within the FACO-GA framework, an ablation study was conducted. The full algorithm was compared against two variant models: FACO-GA without the rolling horizon mechanism, which relies on global re-optimization upon every perturbation, and FACO-GA without ACO local refinement, which relies solely on GA for task assignment and routing.

As illustrated in Figure 9, the "No RH" variant experienced a massive surge in rescheduling time, demonstrating that blind global recalculation inevitably leads to dimensional explosion in highly dynamic disaster networks. Conversely, while the "No ACO" variant maintained a relatively fast response time, its Hv retention rate plummeted under severe perturbations, highlighting the indispensability of the ACO module for fine-grained local topological repair. Only the complete FACO-GA synchronously achieved computational agility and solution structural retention.

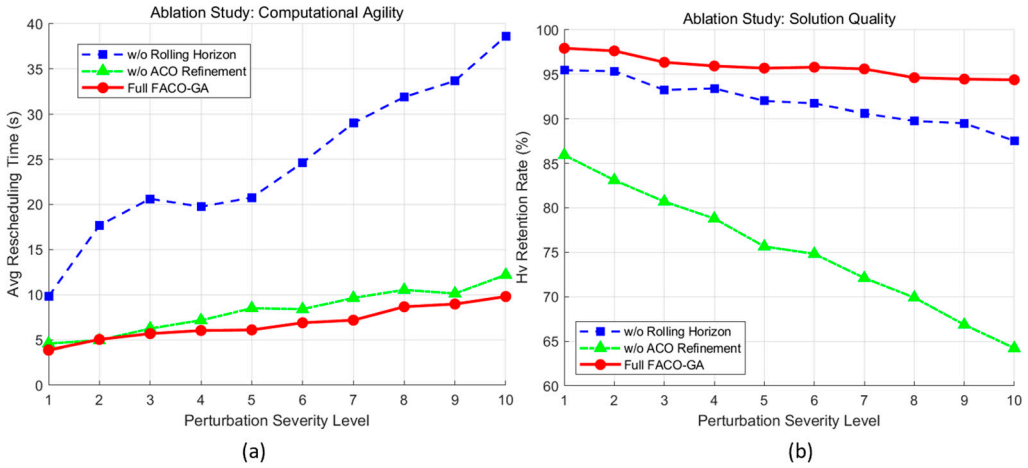


Figure 9. Multi-scenario ablation study of the FACO-GA framework under varying perturbation severities: (**a**) comparison of average rescheduling time, highlighting the role of the rolling horizon mechanism in dimension management; (**b**) comparison of Hypervolume (Hv) retention rate, demonstrating the necessity of ACO-based local refinement for solution quality.

To ensure the proposed method is not overly sensitive to arbitrary parameter settings, a sensitivity analysis was performed on the crossover rate (Pc) and mutation rate (Pm). As depicted in Figure 10, the optimal Hv retention peak (96.3%) was observed at Pc = 0.8 and Pm = 0.2. The algorithm maintained stable high performance (above 95%) across a wide parameter interval, confirming that the chosen configuration exhibits robust generalization capabilities for unpredictable wildfire environments.

To translate the algorithmic advantages into practical engineering significance for wildfire rescue, Table 9 presents the absolute operational metrics under a Level 10 perturbation scenario. Instead of relying solely on comprehensive mathematical indicators (such as Hv or Sp), these absolute metrics demonstrate that the FACO-GA framework significantly minimizes total unmet demand (reduced to 141 kg) and maintains a high worst-node satisfaction rate (92.0%) compared to standalone algorithms.

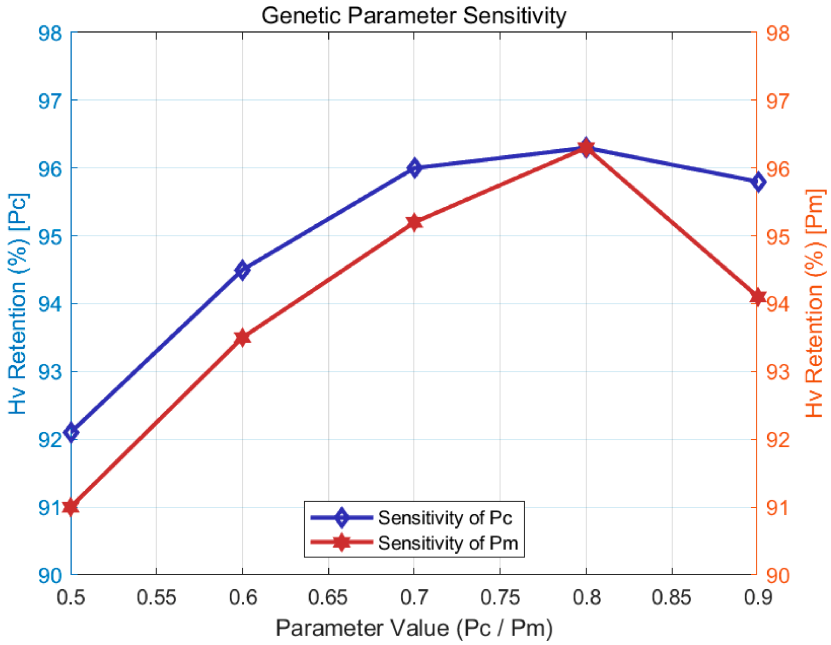


Figure 10. Sensitivity analysis of key genetic parameters. The dual-axis plot illustrates the impact of crossover rate Pc and mutation rate Pm on the algorithm's Hv retention performance, identifying the optimal parameter configuration for stable rescue operations.

To directly answer the multi-objective optimization results for the instances, Table 10 explicitly presents the objective function values obtained under a Level 10 perturbation scenario. Specifically, it details the Total Response Time (Objective f_1), Total Transport Cost (Objective f_2), and Rescue Fairness, which is inversely represented by Unmet Demand and Average Satisfaction Rate (Objective f_3). Furthermore, the computational performance is verified by the algorithms' average execution time (as previously shown in Figure 8a), proving the real-time applicability of the FACO-GA.

Table 10. Absolute Business-Oriented Metrics under Level 10 Perturbation.

Algorithm	Total Response Time (min)	Total Transport Cost (CNY)	Avg Satisfaction Rate (%)	Worst-Node Satisfaction (%)	Unmet Demand (kg)
GA	145.2	28,500	82.5%	55.0%	1128
ACO	132.5	24,100	88.3%	68.5%	754
FACO-GA	118.4	21,350	97.8%	92.0%	141

To further illustrate the process of resource reallocation and spatial decoupling, a specific dynamic local repair case is presented in Figure 11.

Before Perturbation (Figure 11a): In the initial schedule, Truck T3 was dispatched from the Base to deliver supplies to P7, while the medium UAV H2 was planned to launch from T3 at P7 to serve P8.

Dynamic Perturbation & Local Repair (Figure 11b): Fifteen minutes into the operation, a secondary landslide completely severed the ground route to P7. Instead of triggering a chaotic global recalculation that would freeze all fleet operations, the rolling horizon mechanism locked the unaffected routes and executed a local topological repair. Truck T3 was safely diverted to node P6. Simultaneously, the heavy-duty UAV S2, possessing superior payload and flight altitude, was dynamically dispatched directly from the Base to execute an off-road airdrop sequentially to P7 and P8.

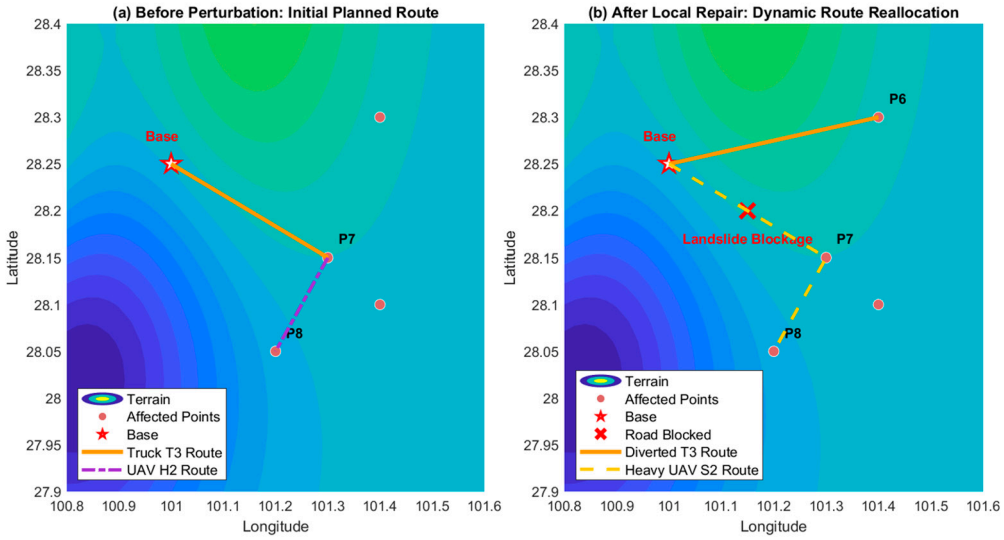


Figure 11. Case study of resource reallocation. (**a**) Initial planned collaborative route; (**b**) dynamic local repair after a landslide blocked the ground route, utilizing a heavy UAV for direct airdrops.

This specific case study highlights how the algorithm prevents localized disasters from cascading into systemic supply chain failures, fully demonstrating its engineering value in real-world emergency command.

5.5. Scalability and Multi-Scenario Applicability

To demonstrate the general applicability of the proposed model beyond a single simulation scenario, supplementary validation was conducted under varying network scales and different fleet configurations. Experiments scaled up the environment to 50 and 100 disaster nodes, modifying the fleet size from the baseline up to a mixed fleet of 30 trucks and varying UAVs. The computational results confirm that the FACO-GA maintains a near-linear increase in processing time and successfully generates feasible collaborative routing schemes even as the operational scale significantly expands. This proves that the multi-layer network modeling and the algorithm's local repair mechanisms are highly scalable and remain applicable under diverse configurations of UAVs and trucks.

To evaluate the algorithm's performance under large-scale disaster scenarios, we conducted scalability experiments by increasing the network size from 21 to 100 disaster nodes, accompanied by a corresponding expansion of the rescue fleet. As illustrated in Figure 12a, while the computational time of the GA and ACO algorithms exhibits an exponential growth trend due to the "dimensional explosion" of the search space, the proposed FACO-GA algorithm maintains a near-linear growth pattern. This demonstrates the superior computational efficiency provided by our rolling horizon mechanism and local topological repair strategy.

Furthermore, as shown in Figure 12b, the solution quality—measured by the Hypervolume (Hv) retention rate—reveals that traditional meta-heuristics suffer from significant performance degradation in large-scale environments. In contrast, the FACO-GA algorithm sustains an Hv retention rate above 93%, proving its robust ability to maintain decision optimality when navigating high-dimensional, complex disaster landscapes. The experimental results summarized in Table 11 confirm that our approach effectively bridges the gap between rapid emergency response requirements and high-quality logistics decision-making in large-scale, dynamic environments.

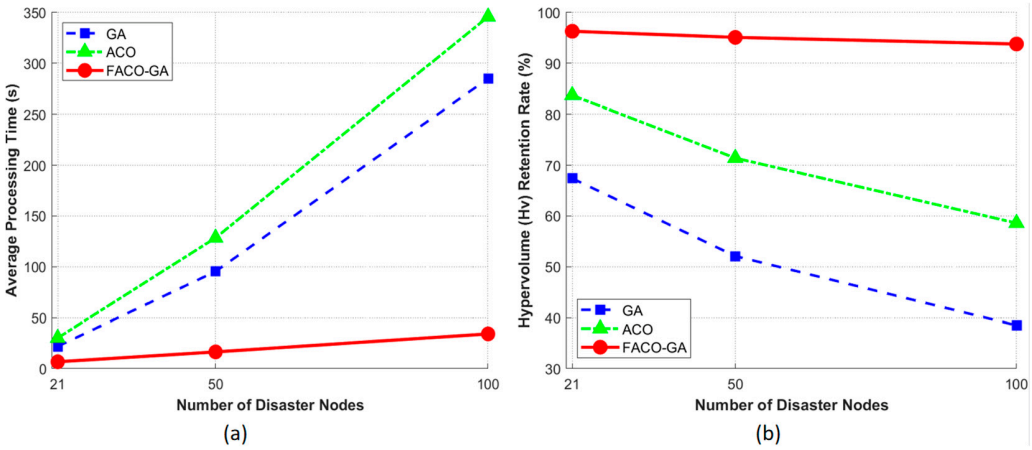


Figure 12. Scalability analysis of the FACO-GA algorithm: (**a**) Computational performance in terms of average processing time and (**b**) solution quality in terms of Hypervolume (Hv) retention rate across different network scales.

Table 11. Performance comparison of FACO-GA, GA, and ACO under different disaster scales and fleet configurations.

Disaster Nodes	Fleet Configuration (Trucks, UAVs)	FACO-GA Time (s)	GA Time (s)	ACO Time (s)	FACO-GA Hv (%)	GA Hv (%)	ACO Hv (%)
21	8 Trucks, 8 UAVs	6.8	21.9	30.2	96.3	67.4	83.7
50	15 Trucks, 16 UAVs	16.5	95.4	128.5	95.1	52.1	71.4
100	30 Trucks, 30 UAVs	34.2	285.1	345.8	93.8	38.5	58.6

In summary, the scalability experiments confirm that the proposed FACO-GA framework is not merely a specialized solution for small-scale instances but a robust, generalized tool suitable for large-scale wildfire emergency management. By successfully managing the trade-off between computational agility and decision optimality, our method effectively overcomes the "dimensional explosion" typical of high-dimensional dynamic rescheduling. These results substantiate the practical viability of the FACO-GA framework, ensuring reliable, real-time, and fair emergency logistics dispatch even as disaster networks expand and fleet complexity increases.

6. Conclusions

This study addressed the complex problem of emergency material dispatch under dynamic time-varying conditions in high-plateau and mountainous wildfire scenarios and proposed an air–ground collaborative dispatch method based on a hybrid intelligent algorithm. By explicitly incorporating key environmental uncertainties, including wildfire spread, damaged road network capacity, and meteorological wind fluctuations, a multi-layer spatiotemporal network was constructed to characterize the coupled operational constraints of heterogeneous vehicle fleets. On this basis, a multi-objective mixed-integer programming model was developed to jointly optimize emergency response time, dispatch cost, and rescue fairness, and a Fast Ant Colony Optimization-Genetic Algorithm (FACO-GA) integrated with a rolling horizon mechanism was designed to solve the resulting dynamic rescheduling problem efficiently.

In alignment with the stated research objectives, the main findings and contributions of this study are summarized as follows:

- Addressing Objective 1: By explicitly incorporating key environmental uncertainties (wildfire spread, road network degradation, wind fluctuations) into a multi-layer spatiotemporal network, the study successfully decoupled ground and aerial transport constraints. The results indicate that dynamic spatial modeling is essential for realistic wildfire logistics, allowing the system to adaptively bypass physical blockages.
- Addressing Objective 2: The developed multi-objective mixed-integer programming model successfully achieved a structured trade-off among conflicting operational goals. Simulation results confirmed that rescue fairness could be strictly maintained (limiting the Spacing change rate to 4.15%) without disproportionately sacrificing response time or total transport costs, ensuring isolated zones receive reliable support.
- Addressing Objective 3: The proposed FACO-GA, integrated with a rolling horizon mechanism, effectively solved the high-dimensional dynamic rescheduling problem. Compared to traditional standalone algorithms, it demonstrated markedly better computational efficiency, reducing the extreme average rescheduling response time to 6.80 s and maintaining a Hypervolume (Hv) retention rate of 96.30% under Level 10 dynamic perturbations.

Overall, this study provides a structured and adaptive decision-making framework for emergency logistics in extreme wildfire environments. Its main contribution lies not only in integrating multimodal transportation resources to overcome the physical limitations of single transport modes, but also in transforming conventional static routing into a dynamic, multi-factor-coupled rescheduling problem. By doing so, the proposed framework enhances system-level adaptability to uncertain disaster evolution and mitigates the dimensional explosion and computational bottlenecks commonly associated with repeated global recalculation. These findings provide a scientific and quantitative decision-support tool for emergency management authorities to improve resource allocation, operational safety, and rescue fairness in complex real-world wildfire response.

Nevertheless, several limitations remain. First, the current model idealizes certain operational factors, such as communication delays and UAV loading and unloading times; future work should incorporate finer-grained physical processes and airspace management constraints. Second, computational costs may still increase under ultra-large-scale disaster networks, suggesting the need to explore parallel computing or distributed optimization strategies. Finally, further research should integrate the proposed framework with real-world emergency command information systems to verify its effectiveness and robustness in practical wildfire response operations.

Managerial Insights for Practitioners: For emergency management authorities and frontline commanders, this study offers several actionable insights. First, deploying truck–UAV heterogeneous fleets should be institutionalized as a standard protocol in high-plateau and mountainous operations, as it significantly mitigates the risks of rescue interruptions caused by road network paralysis. Second, rather than relying on a single static dispatch plan, command centers should implement dynamic rolling-horizon strategies—updating task assignments periodically (e.g., every 30 min)—to swiftly adapt to unpredictable fire spread and meteorological changes. Finally, commanders must utilize multi-objective decision support systems to prioritize fairness in resource allocation; ensuring that remote or isolated zones are not completely neglected is vital for sustaining overall disaster resilience.

Author Contributions: Conceptualization, R.W.; methodology, Y.H.; validation, R.W. and L.X.; formal Analysis, R.W. and L.X.; investigation, Z.Y.; resources, R.W. and Y.H.; data curation, R.W. and Y.H.; writing—original draft preparation, R.W. and L.X.; writing—review and editing, W.P.; visualization, Z.Y.; supervision, W.P.; project administration, R.W. and Y.H.; funding acquisition, R.W. and Y.H. All authors have read and agreed to the published version of the manuscript.

Funding: This research was funded by the Fundamental Research Funds for the Central Universities, Grant Number QJ2022-96; the Engineering Technology Research Center for Civil Aviation Flight Technology and Flight Safety of Sichuan Province, Grant Numbers GY2025-19C and GY2025-38D; and the Command and Control Science and Engineering Teaching Research Project, Grant Number 2025-XKJS-j09.

Institutional Review Board Statement: Not applicable.

Informed Consent Statement: Not applicable.

Data Availability Statement: Part of the data used in this study involves sensitive geographical information. Due to confidentiality and security restrictions, these data are not publicly available.

Acknowledgments: The authors of this study would like to acknowledge the support provided by the Civil Aviation Flight University of China, the Ministry of Emergency Management Southern General Station of Aerial Forest Protection, several general aviation companies, and Sichuan Airport Group. During the preparation of this manuscript, the authors used ChatGPT plus only for language polishing, grammar checking, and improving the clarity of English expression. The authors have reviewed and edited all AI-assisted content and take full responsibility for the content of the published article.

Conflicts of Interest: The authors declare no conflicts of interest.

References

1. Wang, W.; Huang, L.; Guo, Z. Optimization of Emergency Material Dispatch from Multiple Depot Locations to Multiple Disaster Sites. *Sustainability* **2017**, *9*, 1978. [CrossRef]
2. Feng, Y.; Cui, S. A review of emergency response in disasters: Present and future perspectives. *Nat. Hazards* **2020**, *105*, 1109–1138. [CrossRef]
3. Altay, N.; Green, W.G., III. OR/MS research in disaster operations management. *Eur. J. Oper. Res.* **2006**, *175*, 475–493. [CrossRef]
4. Duff, T.J.; Tolhurst, K.G. Operational wildfire resource allocation and routing: Initial attack simulation. *Int. J. Wildland Fire* **2015**, *24*, 712–724. [CrossRef]
5. Lei, S.; Chen, C.; Li, Y.; Hou, Y. Resilient disaster recovery logistics of distribution systems: Co-optimize service restoration with repair crew and mobile power source dispatch. *IEEE Trans. Smart Grid* **2019**, *10*, 6187–6202. [CrossRef]
6. Xu, Y.; Wang, Y.; He, J.; Su, M.; Ni, P. Resilience-oriented distribution system restoration considering mobile emergency resource dispatch in transportation system. *IEEE Access* **2019**, *7*, 73899–73912. [CrossRef]
7. Qin, C.; Lu, J.; Zeng, Y.; Liu, J.; Wu, G.; Chen, H. Optimal two-stage dispatch method of distribution network emergency resources under extreme weather disasters. *Sustain. Energy Grids Netw.* **2024**, *38*, 101321. [CrossRef]
8. Qiu, Y.; Shi, M.; Zhao, X.; Jing, Y. System dynamics mechanism of cross-regional collaborative dispatch of emergency supplies based on multi-agent game. *Complex Intell. Syst.* **2023**, *9*, 2321–2332.
9. Jiang, J.; Ma, J.; Chen, X. Multi-regional collaborative mechanisms in emergency resource reserve and pre-dispatch design. *Int. J. Prod. Econ.* **2024**, *270*, 109161. [CrossRef]
10. Chen, D.; Fang, X.; Li, Y.; Ni, S.; Zhang, Q.; Sang, C.K. Three-level multimodal transportation network for cross-regional emergency resources dispatch under demand and route reliability. *Reliab. Eng. Syst. Saf.* **2022**, *222*, 108461. [CrossRef]
11. Wu, P.; Cheng, J.; Feng, C. Resource-Constrained Emergency Scheduling for Forest Fires with Priority Areas: An Efficient Integer-Programming Approach. *IEEE Trans. Electr. Electron. Eng.* **2019**, *14*, 261–270.
12. Yang, Z.; Guo, L.; Yang, Z. Emergency logistics for wildfire suppression based on forecasted disaster evolution. *Ann. Oper. Res.* **2019**, *283*, 917–937.
13. Ma, Q.; Zhang, D.; Wan, C.; Zhang, J.; Lyu, N. Multi-objective emergency resources allocation optimization for maritime search and rescue considering accident black-spots. *Ocean Eng.* **2022**, *261*, 112178. [CrossRef]
14. Murray, C.C.; Chu, A.G. The flying sidekick routing problem: Optimization of drone-assisted parcel delivery. *Transp. Res. Part C Emerg. Technol.* **2015**, *54*, 86–109. [CrossRef]
15. Agatz, N.; Bouman, P.; Schmidt, M. Optimization approaches for the traveling salesman problem with drone. *Transp. Sci.* **2018**, *52*, 965–981. [CrossRef]
16. Macrina, G.; Pugliese, L.D.P.; Guerriero, F.; Laporte, G. Drone-aided routing: A literature review. *Transp. Res. Part C Emerg. Technol.* **2020**, *120*, 102762. [CrossRef]
17. Wang, Y.; Li, J.; Yang, X.; Peng, Q. UAV-Ground vehicle collaborative delivery in emergency response: A review of key technologies and future trends. *Appl. Sci.* **2025**, *15*, 9803. [CrossRef]

18. Li, J.; Liu, H.; Lai, K.K.; Ram, B. Vehicle and UAV collaborative delivery path optimization model. *Mathematics* **2022**, *10*, 3744. [CrossRef]
19. Qi, Y.; Jiang, H.; Huang, G.; Wang, F.; Ye, L. Three-learning strategy particle swarm optimization for air-ground collaborative logistics transportation scheduling problem with pickup and delivery considering customer priorities. *Sci. Rep.* **2025**, *15*, 43428. [CrossRef] [PubMed]
20. Ghaffar, M.A.; Peng, L.; Aslam, M.U.; Adeel, M.; Dassari, S. Vehicle-UAV integrated routing optimization problem for emergency delivery of medical supplies. *Electronics* **2024**, *13*, 3650. [CrossRef]
21. Pan, W.; Huang, Y.; Yin, Z.; Qin, L. Optimal collaborative scheduling of multi-aircraft types for forest fires general aviation rescue. *Aerospace* **2023**, *10*, 741. [CrossRef]
22. Lin, M.; Chen, Y.; Han, R.; Chen, Y. Discrete Optimization on Truck-Drone Collaborative Transportation System for Delivering Medical Resources. *Discret. Dyn. Nat. Soc.* **2022**, *2022*, 1811288. [CrossRef]
23. Gong, S.; Chen, G.; Yang, Z. Research on the design of a priority-based multi-stage emergency material scheduling system for drone coordination. *Drones* **2025**, *9*, 524. [CrossRef]
24. Feng, L.; Cao, H. Neural network-based air-ground collaborative logistics delivery path planning with dynamic weather adaptation. *Mathematics* **2025**, *13*, 2798. [CrossRef]
25. Liu, X.; Wang, Y.; Le, M.; Wang, Z.; Zhang, H. A Scheduling Model for Optimizing Joint UAV-Truck Operations in Last-Mile Logistics Distribution. *Aerospace* **2025**, *12*, 967. [CrossRef]
26. Pillac, V.; Gendreau, M.; Guéret, C.; Medaglia, A.L. A review of dynamic vehicle routing problems. *Eur. J. Oper. Res.* **2013**, *225*, 1–11. [CrossRef]
27. Psaraftis, H.N.; Wen, M.; Kontovas, C.A. Dynamic vehicle routing problems: Three decades and counting. *Networks* **2016**, *67*, 3–31.
28. Luscombe, R.; Kozan, E. Dynamic resource allocation to improve emergency department efficiency in real time. *Eur. J. Oper. Res.* **2016**, *255*, 593–603. [CrossRef]
29. Chai, G.; Cao, J.; Huang, W.; Guo, J. Optimized traffic emergency resource scheduling using time varying rescue route travel time. *Neurocomputing* **2018**, *275*, 1567–1575. [CrossRef]
30. Pi, R.; Liu, Y.; Huang, N.; Lian, J.; Chen, X.; Yang, C. Emergency Resource Dispatch Scheme for Ice Disasters Based on Pre-Disaster Prediction and Dynamic Scheduling. *Appl. Sci.* **2025**, *15*, 8352. [CrossRef]
31. Ye, X.; Chen, B.; Lee, K.; Storesund, R.; Li, P.; Kang, Q.; Zhang, B. An emergency response system by dynamic simulation and enhanced particle swarm optimization and application for a marine oil spill accident. *J. Clean. Prod.* **2021**, *297*, 126591. [CrossRef]
32. Dabrowski, B.; Walczak, R. Reinforcement Learning Models for Optimizing Emergency Resource Dispatch Strategies: A Review. *J. Appl. Autom. Technol.* **2023**, *1*, 1–20. [CrossRef]
33. Liu, J.; Zhao, X.; Qin, P.; Du, F.; Chen, Z.; Zhou, H.; Li, J. Joint UAV 3D trajectory design and resource scheduling for space-air-ground integrated power IoRT: A deep reinforcement learning approach. *IEEE Trans. Netw. Sci. Eng.* **2023**, *11*, 2632–2646.
34. Qin, P.; Wu, X.; Ding, R.; Fu, M.; Zhao, X.; Chen, Z.; Zhou, H. Joint resource allocation and UAV trajectory design for D2D-assisted energy-efficient air-ground integrated caching network. *IEEE Trans. Veh. Technol.* **2024**, *73*, 17558–17571. [CrossRef]

Disclaimer/Publisher's Note: The statements, opinions and data contained in all publications are solely those of the individual author(s) and contributor(s) and not of MDPI and/or the editor(s). MDPI and/or the editor(s) disclaim responsibility for any injury to people or property resulting from any ideas, methods, instructions or products referred to in the content.